J. D. Crow

(GaAl)As Laser Requirements for Local Attached Data Link Applications

The characteristics of (GaAl)As double heterostructure stripe contact injection lasers as they relate to applications in fiber optic data transmission systems are reviewed. The laser characteristics are treated as optical, electrical, thermal, and mechanical interfaces to the system in order to emphasize the necessity of designing devices as a functional part of a system or subsystem. It is concluded that the laser is generally well suited as an optical source in a card-mountable hybrid module transmitter for data links up to a few km and ≈100 Mbit/s data rates. Areas requiring further development include lowering of the laser threshold current, improving the modal stability, packaging the laser with electronics and fiber optic transmission lines, and improving the laser lifetime under varying ambient temperature conditions.

Introduction

One of the major applications of lasers is in communications, as anticipated at the inception of laser research in the late 1950s [1] and evidenced by continued attention throughout the 1960s [2]. A major deterrent to the rapid development of optical communication during this period was the lack of a reliable low-loss transmission medium. With the advent of low-loss optical fibers in 1970 [3], development of fiber optic communication systems became a major concern for the telecommunications industry. Today, it is one of the most rapidly advancing fields in electronics. Fiber and optical cable production has reached the point where field installation has been extensively demonstrated and costs are competitive with coaxial and twisted-wire copper cable in some applications [4]. Component development has also advanced rapidly; there are prototype products on the market for connectors, optical sources and detectors, taps, and supporting electronics.

A key component in fiber optic communication systems is the optical source; the primary candidates are the semiconductor light-emitting diode (LED) and the injection laser. This paper discusses injection lasers, concentrating on lasers of the double heterostructure type that use epitaxially grown layers of GaAs and $Ga_{1-x}Al_xAs$. The GaAs injection laser has made considerable progress since its inception in 1962 [5], with continuous wave (cw) room-temperature operation being demonstrated in 1970 [6], and projected lifetimes in excess of 10^6 hours measured in 1977 [7].

This paper reviews the requirements on injection lasers for use in optical links that transmit digital information. Rather than treating the laser as a device *per se* or in the general context of optical communications [8], the discussion is limited to the environment found in computer industry links, *i.e.*, the interfaces to the laser and constraints on the laser due to that environment. It is shown how specific applications can influence the tradeoffs necessary to fit a device into a system. Computer networks connected through common carrier systems, such as telephone, satellite, or microwave networks, are not discussed. Rather, a treatment is given of applications to the "local attached system." The computer industry "local" data transmission networks are those found in the machine rooms of large computer systems and those distributed around the building or plant site of data processing (DP) users [9]. Typical data rates and transmission distances required for today's applications are shown in Fig. 1 [9]. Terminal networks have longer links between nodes, but modest data rate requirements; computer "machine room" networks use higher bandwidths (if serialized), but shorter distances. Distributed DP networks tend to fall in between. These networks interconnect many pieces of equipment of varying cost, size, and performance characteristics. The major hardware costs in a DP system are those involving equipment, not cable. Thus, costs added to each piece of equipment, such as for an electro-optic interface for a fiber optical network, could add to the overall system costs even though fiber optic cables might be less expensive than their electrical counterparts. (This is to be contrasted to the telecommunications industry environment where the cable costs dominate equipment costs.) The DP equipment contains digital electronics packaged in modules on wiring boards. The electro-optic interfaces must fit onto these modules or boards with minimum alteration if the use of fiber optic technology is to give both cost and performance advantages.

A typical fiber optic link consists of driver electronics, an optical source, a coupling mechanism to the fiber optic cable, the cable, coupling to the photodetector, and the receiver electronics. The GaAs laser source must interface directly with the electrical and optical components of the transmitter and must be compatible with their thermal and mechanical constraints. The laser must also satisfy the optical performance requirements imposed by the system.

The double heterostructure (DH) laser, consisting of epitaxially grown layers of GaAs and $Ga_{1-x}Al_xAs$, has properties that meet many of the requirements of both fiber optic transmission medium and DP equipment. Fundamental characteristics key to motivating this laser's development are as follows: a range of emission wavelengths well matched to low attenuation bands in the fiber, the ability to be pumped and directly modulated by electrical current sources, and the ability to be fabricated in a batch mode using many of the planar processes developed for the silicon-based electronics industry. The (GaAl)As DH laser can be fabricated in a number of configurations [8] such as mesa structures or grating coupled structures. The one with the best present overall performance in fiber optic systems uses parallel cleaved end facets to form a lasing cavity and a current-confining stripe along the length of the cavity to localize the volume of crystal pumped by current injection. See Fig. 2 and Fig. 1 of a companion paper in this issue by Lynch *et al.* [10]. The stripe laser configuration has a demonstrated lifetime of over 35 000 hours operating cw at room temperature [11] and is therefore a suitable candidate for applications in DP equipment with a product life of around five years. The optimization of the stripe contact DH injection laser for fiber optic data-link applications is the focus of the remainder of this paper.

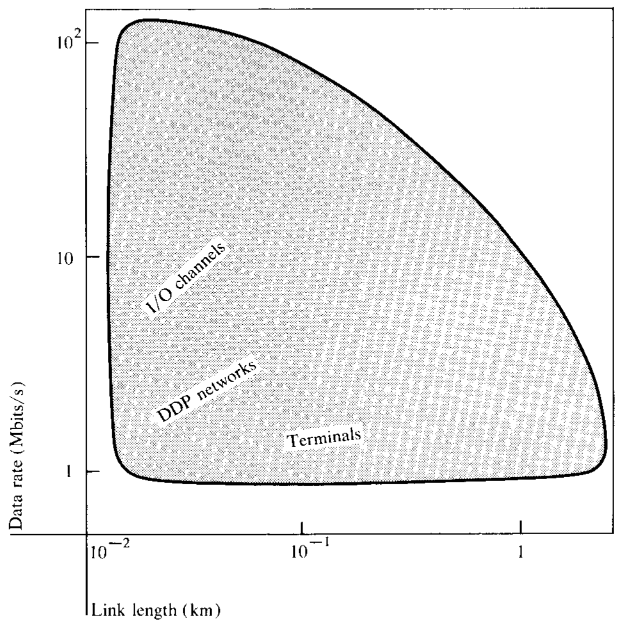

Figure 1 Typical data rates and link lengths for existing computer industry local data transmission applications [9].

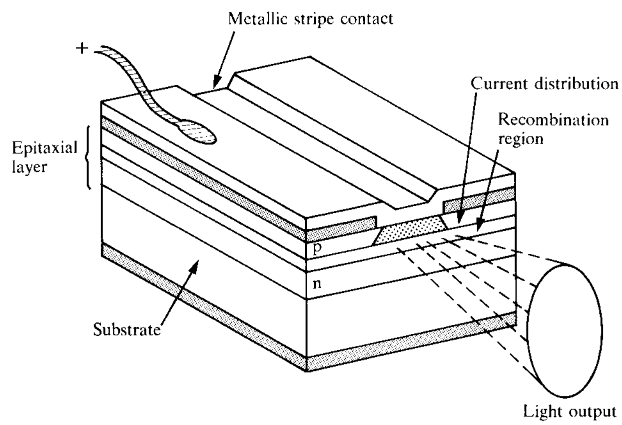

Figure 2 Schematic of a typical stripe-geometry laser. The stripe is mounted on the heat sink and the laser light is emitted from the cleaved end facets in the recombination region under the stripe.

The following sections discuss the optical, electrical, and thermal interface requirements for the laser and review how present designs and packaging meet these requirements.

Optical interface

The laser must efficiently couple optical power to the fiber transmission line at a wavelength corresponding to

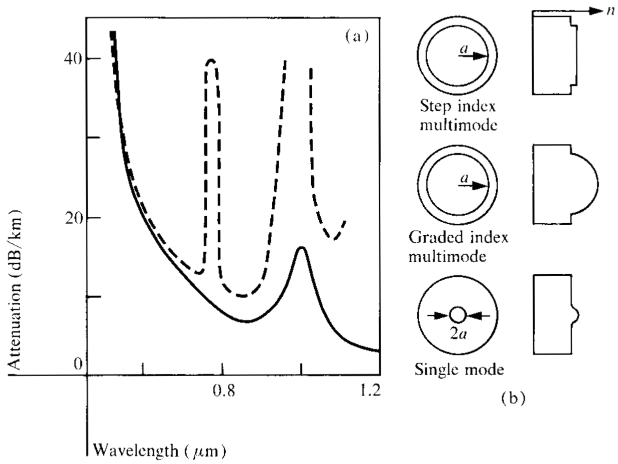

Figure 3 (a) Optical attenuation *vs* wavelength of plastic-clad silica (PCS) (- - -) and doped fused silica (——) fibers. (b) Fiber cross-sectional views (left) and refractive index profiles (right) of fibers; a is the core radius, n is the radial distance.

low optical attenuation in the fiber. The fibers most likely to be used with lasers in data-link applications have light-guiding cores of fused silica or doped fused silica and exhibit low signal attenuations and high bandwidths [4]. Typical attenuation spectra for these fibers are shown in Fig. 3(a) for commercially available all-glass and plastic-clad glass fibers. Both types of fiber have low-loss windows in the 0.8-μm to 0.9-μm wavelength range, which corresponds to the optical emission wavelengths of $Ga_{1-x}Al_xAs$ with $x \lesssim 10\%$.

Coupling efficiency between laser and fiber depends on the laser optical beam shape and divergence, and the fiber core area and acceptance angle. Figure 3(b) shows the fiber cross-sectional views and the refractive index profiles for plastic-clad silica (PCS) and doped fused silica fibers. The doped silica fibers can have either a step or a graded index profile, with typical values for the core radius a of 30 μm and for Δn (n = radial distance) of 0.013; PCS has a step index profile with typical values for a and Δn of 100 μm and 0.031. For the data rate and distance requirements of Fig. 1, multimode fibers are adequate, and the core radius is typically 25 to 150 μm. The acceptance angle is determined by the relative indices of refraction for the core and cladding materials and by the radial profile of this index. For abrupt index changes at the core-cladding boundary, typical acceptance half-angle values are $\approx 9°$ for doped silica fibers and 20° for plastic-clad silica fibers. For near-parabolic radial profiles of index of refraction, the acceptance angle depends on the radial extent of the laser beam; this can effectively reduce the acceptance angle by as much as one-half when compared to a step index fiber of the same core and cladding materials [4]. For maximum coupling efficiency, the laser emission must be imaged onto the fiber end face with a cross-sectional spot size less than the effective core cross section and a beam divergence less than the acceptance angle.

The laser output beam size and divergence depend on the emission aperture of the laser cavity. Figure 2 shows schematically how the laser light, emitted from the end facet of the device in the region near the p-n junction and under the stripe, is asymmetric due to the difference in aperture dimensions perpendicular and parallel to the p-n junction plane. The laser aperture dimension in the direction perpendicular to the junction is determined by the optical waveguide formed by refractive index discontinuities between the recombination region and the surrounding (GaAl)As regions. With the amount of Al in the recombination region chosen for wavelength optimization (Al_x, $x \approx 0.1$), the Al concentration in the sandwiching epilayers is chosen in conjunction with the active region thickness d, so that the waveguide perpendicular to the junction is limited to single mode propagation ($x \approx 0.3$). Single transverse mode output is desirable because this mode can be coupled most efficiently to fibers. The thickness of the active region is chosen as a compromise between low threshold current density [see Fig. 4(a)] [12, 13], and the ability to reliably grow thin active layers. Typically, sandwich layer Al concentrations are $x = 0.3$, leading to $d \lesssim 0.3$ μm for single transverse mode operation. However, notice in Fig. 4(b) [8] that with d typically 0.2 μm and $x = 0.3$, the beam divergence perpendicular to the junction is approximately 45° (FWHM), which far exceeds the acceptance angle of low-loss fibers. Currently, this mismatch is being corrected by the use of external optics to collimate the beam (discussed further in the packaging section).

In stripe-geometry lasers, the optical emission parallel to the junction is defined by the optical gain distribution along the junction. The laser gain distribution along the p-n junction can be controlled by confining the width of the junction through which current passes by means of oxide stripes on the surface as shown in Fig. 2, by ion-implanting or proton-bombarding regions adjacent to the stripe to raise the material resistivity, or by diffusing dopants along the stripe [8]. At low optical outputs, single transverse mode behavior has been widely demonstrated [14]. The far-field divergence of the resultant beam parallel to the p-n junction is about 10° (FWHM) and is easily captured by the fiber. As drive current increases, the effective guide width increases due to current spread [15] and lateral diffusion of injected carriers in the active layer to regions outside the stripe [16], and the transverse emission pattern can become multimoded. This results in increased far-field divergence and near-field spot size, and lowers the coupling efficiency to low numerical aperture (NA) fibers. Defects in the active region can lead to localized filaments [14, 17]. These result in unstable optical beam properties, including large (≈ stripe width) lateral translations of the emission near field, and can drastically affect coupling efficiencies to fibers.

In single transverse mode operation, the laser is well suited to efficient coupling to the multimode silica fiber of Fig. 3, except for the laser beam divergence perpendicular to the junction. Coupling efficiencies of 20–35% have been reported for fibers butted to lasers [18, 19]. This efficiency can be increased to 55% [19] by melting the fiber end to form a hemispherical lens, while coupling efficiencies up to 80% are obtained [20] by using a piece of fiber as a cylindrical lens to compensate for both laser beam asymmetry and large perpendicular beam divergence.

The optical power required from a laser is system dependent. The functional requirement is to have enough signal power at every optical receiver in the system to allow for electrical signal regeneration at an acceptable signal-to-noise ratio or bit error rate. In addition to the laser-to-fiber coupling efficiency, the power required depends on system data rates, noise sources, and the network configuration (*e.g.*, transmission line length, number of connectors, taps, switches, etc.). C. K. Kao and J. E. Goell [21] give one approach to designing fiber optic links based on optical power budgets. Generally, point-to-point links in the performance range indicated in Fig. 1 can use lasers emitting in the 1-3-mW range. Links containing many connectors, or networks of links with passive signal splitting devices, however, place added power requirements on the laser transmitter, *i.e.*, in compensating for the added system loss. In these environments, more laser power in the fiber translates to more passive taps in the network. Also, higher data rates place added power demands on laser transmitters because of the reduced signal-to-noise performance of the receiver. In short, more optical power is always useful either in simplifying the electronics, giving lower error rates, or making more complex networks possible. Increased optical output can lead to catastrophic device failure [22] and results in shorter device lifetime [23]. Power limitations due to catastrophic device failure via facet damage can be alleviated by coating the facets with dielectrics [24] and by making the emission aperture as large as possible without sacrificing single transverse mode operation. With dielectric-coated facets, metallic or dielectric reflectors on the end facets can be used to optimize unidirectional output power from the laser cavity. H. Imai *et al.* [25] mention that laser lifetime decreases as the square root of the output power at 70°C. Recall that increased optical power can result in multimode or filamentary behavior, so that lower coupling efficiency to fibers results. Strong lateral confinement techniques [8] can suppress multimode behavior at higher power levels, but very narrow (1-3-μm) effective guide widths are needed and these increase the probability of facet damage.

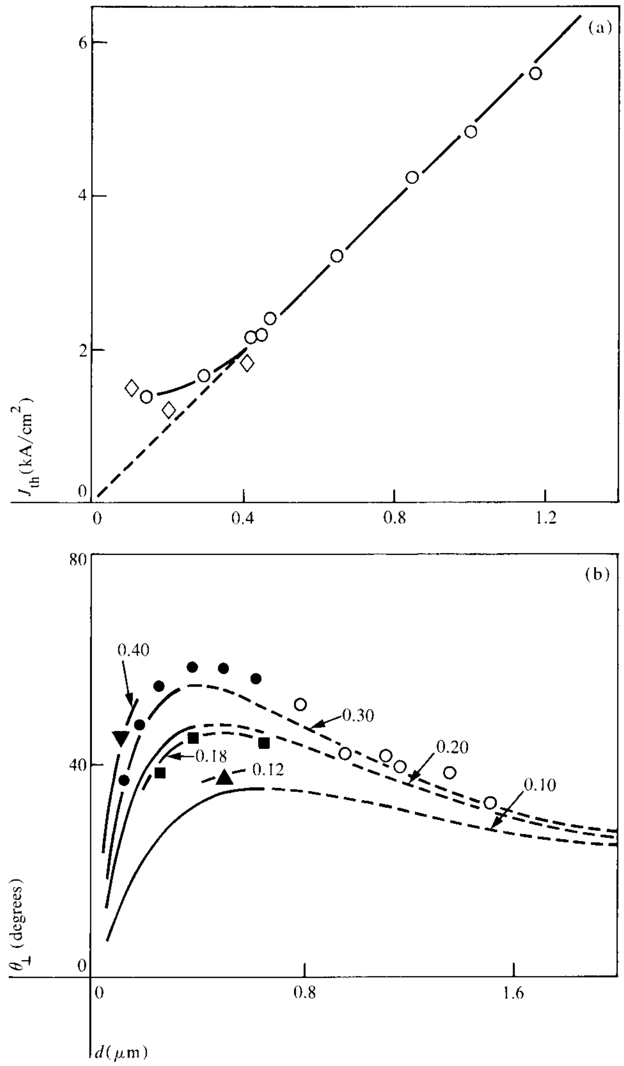

Figure 4 (a) Threshold current density J_{th} as a function of recombination region thickness d. The ○ are from Ref. [13]; the ◇, from Ref. [10] (devices with similar dopings and epilayer compositions); $J_{th}/d \approx 4.9$ kA/cm^2-μm. (b) Divergence of the laser output beam perpendicular ($\theta_\perp$) to the p-n junction plane (*i.e.*, full beam width between half-power points) as a function of active layer thickness and relative difference in the Al concentration (see numbers on figure) between the active region and the surrounding epilayers. Data compiled from many authors' work [8].

The laser linewidth can influence the data-link rate by means of fiber pulse spread. Figure 5 [26] plots pulse

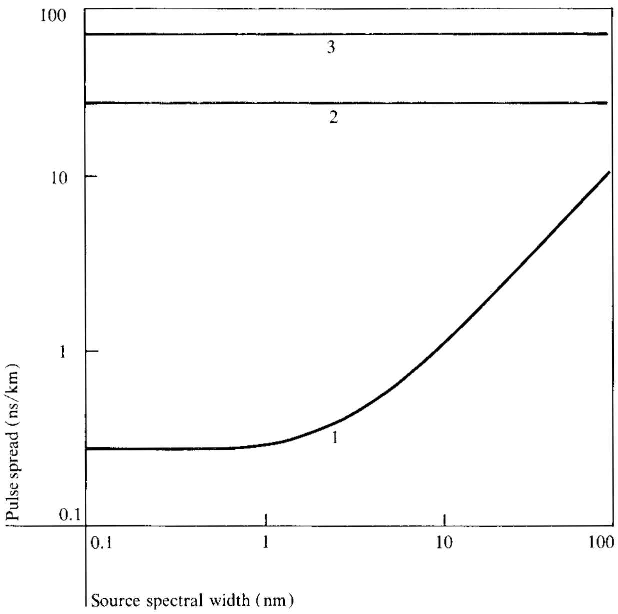

Figure 5 The spread of an input pulse to a fiber optic transmission line as a function of the spectral width of the input pulse. Lasers are nominally 1-2 nm in linewidth. Curve 1 is for a "practical" graded index, doped silica fiber with $\Delta = \Delta n/n = 0.01$ [numerical aperture (NA) = 0.2]; curve 2, for a step index, doped silica fiber with the same NA; and curve 3, for a step index, plastic-clad silica fiber with $\Delta = 0.03$ (NA = 0.36) [26].

spread *vs.* spectral linewidth for all-glass graded and step index fibers, and plastic-clad silica step index fibers. For a (GaAl)As laser, typical linewidths are 1-2 nm, so that the pulse spread is limited almost entirely by modal propagation effects in the fiber itself and not by material dispersion, which depends on the source linewidth.

Electrical interface

The electrical interface between the laser and transmitter electronics provides the laser with the ac data stream, dc bias power, and device control signals. A common mode of device operation is to bias the laser to an operating point above the lasing threshold current and then add an ac modulation current to the operating current, as shown in Fig. 6 (see [11]). Biasing above threshold lowers the ac modulation currents necessary and improves device speed.

The dc requirements are to supply currents to exceed I_{th} at voltages sufficient to forward bias the p-n junction [*i.e.*, $V_b \geq IR + V_0$, where R is the ohmic resistance of the device and its contact (typically 1 Ω) and V_0 is the junction voltage (typically 1.5 V)]. Threshold current depends on threshold current density J_{th} and junction area. Present oxide stripe devices have $J_{th} \approx 1.5$ kA/cm^2, and the effective pumped region of the junction is typically 20 μm in width and 300 μm in length, leading to threshold currents of ≈90 mA and applied voltages of ≈1.7 V. The ac current modulation is determined by the optical power modulation depth required for a specified signal-to-noise ratio at the receiver and the differential quantum efficiency η, which is the slope of the light output *vs* current curve of Fig. 6; *i.e.*, $\eta = P_L/V_0(I - I_{th})$. Typically $\eta \approx 0.5$, so that a 10-mW modulation depth requires about 13 mA of signal current.

The electronics available in DP equipment are primarily integrated circuits. Using emitter-coupled logic (ECL) as an example of a likely electronic interface to the laser [27], we note that ac current swings in the tens of mA per gate are available, with ac voltage swings of ≈1 V at the data rates shown in Fig. 1. Also available are dc power supplies of ±5 V. Thus, it is possible to use logic line drivers and logic family power supplies to provide electrical signal and power to the laser.

The maximum modulation rate of the laser is determined by turn-on delays (typically a few ns) and relaxation oscillations (also lasting a few ns) [28]. By biasing to slightly above threshold, these effects are suppressed. The interaction between the carrier population inversion and the optical field in the cavity (the cause of the relaxation oscillations) can still result in noise resonance; this is typically around 1 GHz, which is above the data rates of interest on Fig. 1.

Thermal interface

The thermal characteristics of the GaAs DH laser influence its optical characteristics and also must be considered in designing the device structure. The laser wavelength, threshold current I_{th}, and differential quantum efficiency η all depend upon the p-n junction temperature T. Junction temperature is determined by the ambient temperature surrounding the laser and the temperature rise associated with heat generation in the electrical to optical transduction process. The electrical components in DP equipment are expected to function in an ambient of 0 to 75°C [29]; thus, the laser should operate in this environment also.

The laser wavelength variation over this temperature range (≈30 nm at 0.4 nm/°C [8]) does not affect link attenuation or bandwidth significantly; however, links that use wavelength multiplexing to increase the information-carrying capacity of the fibers, and the corresponding wavelength-dependent taps, splitters, and concentrators, can be severely affected by 30-nm wavelength shifts. Grating reflectors can act to stabilize laser emission wavelength against temperature. About an order of magnitude (*i.e.*, 0.04 nm/°C) reduction is predicted [4].

Under constant drive-current conditions (see Fig. 6) a modest temperature variation can have a severe effect on the optical output power, and can even quench the lasing process. Some means of compensating for temperature shift is necessary. One approach is to control the laser junction temperature in spite of varying ambient temperature by packaging the laser with a cooling device. The other approach is to change the drive current through the device to adjust for temperature effects and maintain constant optical output power. In either case the optical output power is the parameter held constant; thus the optical output is monitored with a photodiode and a feedback control signal is generated to control either cooler power or drive current. All thermal and some current control techniques regulate average optical output, but current controllers can also maintain an average optical output in proportion to the average electrical data pulse pattern input, or maintain both peak power output and modulation depth.

R. Laff *et al.* [30] discuss how thermoelectric coolers are used in optical feedback loops to control average optical output power. The advantage of temperature control is that it is a negative feedback technique. That is, as optical output drops due to junction temperature rise or aging, the cooler lowers the "effective" ambient temperature and thus lowers the junction temperature to its original value. Another advantage of active device cooling is that the junction temperature is maintained at as low a value as practical. High-temperature lifetime tests on lasers indicate an average lifetime degraded by 65 times at 70°C over that at 22°C [23]. However, thermoelectric coolers are larger and more expensive than the electronic components in the modular transmitter environment and require currents varying over hundreds of mA to provide sufficient cooling capacity.

Use of the laser drive current to control the optical output has advantages: It is a faster means of control, it is able to account for data patterning effects, and it can be incorporated into the modular environment of data transmission equipment. The magnitude of current change necessary and the speed with which the control circuit must respond to optical output fluctuations determine the speed-power product of the control electronics and their complexity. This circuitry can become a significant heat source itself, and must be included in determining the heat generated by the laser transmitter if it is located on the same module as the laser. A disadvantage of current control is that it can lead to uncontrolled feedback; *i.e.*, increasing the drive current increases the junction temperature, which further reduces the optical output and thus requires further current increase, leading to potential feedback instability.

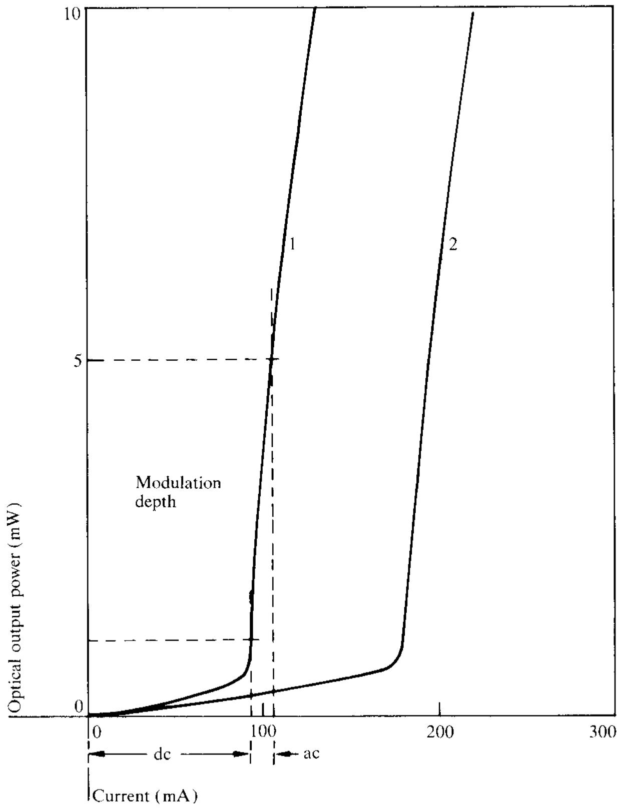

Figure 6 The single-facet optical output power *vs* drive current for a typical IBM injection laser at 20°C (curve 1) and 80°C (curve 2). The dashed lines indicate a typical dc bias and ac modulation current applied to the device; this results in an optical modulation depth >3 mW. Note that a 60°C shift in temperature would quench lasing if the total current were <175 mA.

It is desirable from the feedback-control viewpoint to design a laser with minimal variations of I_{th} and η with temperature and to fabricate and package with minimal thermal resistance R_{th}. Weak carrier confinement across the laser junction has been shown to lead to sensitivities of laser I_{th} and η to temperature [31, 32]. Carrier confinement is determined by the heterojunction step height (change in relative Al content) and the material doping. For heterojunction steps $\geq$ 25%, (GaAl)As layer doping $< 10^{18}/cm^3$, and a 10-μm stripe width.

$$I'_{th} \equiv I_{th}(65°C)/I_{th}(10°C) \leq 1.5$$

is commonly reported [8, 32] and the slope of I_{th} *vs* T is approximately linear. The external differential efficiency η for these devices decreases approximately linearly with increasing temperature, but the slope varies considerably in the literature. Existing devices have

$$\eta' \equiv \eta(65°C)/\eta(10°C) \approx 0.8\text{–}1.0.$$

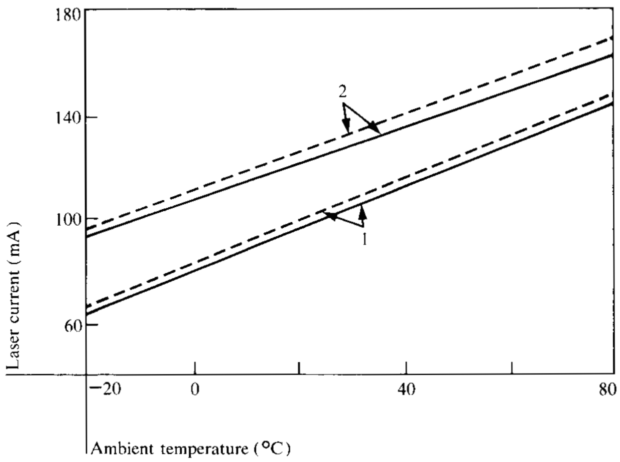

Figure 7 Total drive current required for the specified single-facet optical output P_L of 1 mW (curves 1) and 10 mW (curves 2) as a function of ambient temperature and package thermal resistance (——, 50 Ω; - - -, 75 Ω). The sensitivities of I_{th} and the differential quantum efficiency were assumed to be linear with slopes I'_{th} = 1.5 and η' = 0.8, respectively (see text).

The thermal resistance of lasers is a function of the device geometry, the bond quality, and the thermal conductivity of the materials in the epilayers, bond metallurgy, and heat sink [32, 33]. For devices nominally of 300-μm stripe length, 10-μm stripe width, and with a Cu heat sink, $R_{th} \approx$ 25°C/W [33]. Devices that have a larger junction area (*i.e.*, active region width times laser length) have lower thermal resistances, but at the expense of higher I_{th} and a multitransverse mode output.

If current feedback control techniques are used, it is important to determine whether the bias and modulation currents required to maintain a controlled optical output are achievable with integrated electronics. An estimate of the drive current change *vs* ambient temperature change at two optical output powers (single-facet) and two different room-temperature I_{th} devices is shown in Fig. 7 [34]. We see that if the laser [I_{th}(25°C) = 90 mA] is packaged such that its junction to ambient thermal resistance is 50–75°C/W [35] and the desired optical power is 10 mW, the bias point will vary between 100 and 160 mA as the ambient fluctuates between $0 < T_a < 75$°C. This magnitude of current control would be possible from circuits in an ECL logic family, but it may require operating logic line drivers in parallel and be a significant heat source itself. Note that the thermal resistance of the laser packaging does not critically influence operating currents required. Figure 7 also illustrates how a drop in I_{th} (room temperature) from 90 to 50 mA allows a significant reduction in both bias current and controller current range. This is a strong motivation towards the development of low-threshold laser structures, especially as modulation rates increase and available current modulation amplitudes decrease.

Controlling the optical output in varying ambient temperatures is only one aspect of the thermal interface. The other concerns are whether the laser package can dissipate the heat generated by the laser and its controller into that ambient, and the effect of temperature on laser lifetime. Heat dissipation is discussed again in the next section. S. Ritchie *et al.* [36] discuss degradation mechanisms that can be accelerated by high-temperature operation and Refs. [7] and [37] present data on how mean lifetime is reduced by allowing junction temperatures to rise to 70°C.

Laser packaging

To be useful for optical communications applications, the GaAs laser must be incorporated into an optical source package in such a way that its optical performance is not compromised while its electrical and thermal requirements are met. The packaging should be inexpensive, reliable, and lend itself to automatic assembly techniques. In the case of GaAs DH lasers, this is a real challenge because of highly divergent optical beam characteristics, high thermal power densities to dissipate, the sensitivity of device reliability to strain, and the diversity of materials involved (*e.g.*, GaAs, Si, metals, glass fibers). Recall that we are presuming the environment for this package to be a printed circuit card containing hybrid and integrated circuit electronics that share common power supplies, cooling, etc. In this environment, the space needed for the laser package can directly influence system cost, so another goal is to keep the laser packaging as small as possible.

Large laser beam divergence means that the output beam must be collected by an optical system very close to the laser facet if large (and hence expensive) optical components and a large package are to be avoided. Current approaches involve mounting the laser on a heat sink very close to an edge and then mounting the optical system just beyond the edge. The optical system may be the fiber itself [18], the fiber with a melted tip [19], or a miniature cylindrical lens followed by the fiber [20]. Typical coupling efficiencies into low-NA, multimode, doped silica fibers using the above approaches are 25, 50, and 70%, respectively. The increased coupling efficiency in the last two approaches is accompanied by a decrease in positional tolerance of the optical components with respect to the laser emission aperture. A transverse displacement between the cleaved end of a fiber and the emission facet of the laser of a distance equal to the core radius (*e.g.*, ≈ ±25 μm) results in a 50% reduction in coupling efficiency. With lensed surfaces, this tolerance drops to typically one-fifth the core radius (*e.g.*, $\approx$ $\pm 6\,\mu$m) [20]. Therefore, if high laser-to-fiber coupling efficiency is desired, the package must provide accurate alignment of the optical components to the laser. Two approaches to providing accurate alignment have been reported. One involves micromanipulating the optical components in front of the laser while it is operating, and optimizing the monitored optical output of the fiber. When optimum coupling is achieved, the optics are glued in place with epoxy [19]. This technique assures initial alignment, but its reliability and assembly cost are concerns. The other approach is to use accurately fabricated grooves on a common substrate to align the optics with the laser. This technique lends itself to less expensive assembly and should yield greater alignment reliability, but it presumes that the grooves and optical components can be made with sufficient precision to allow self-alignment techniques to work. With etched grooves in single-crystal Si, alignment accuracies better than $\pm 3\ \mu$m have been demonstrated [20].

Thermal and mechanical contact between the device and the package substrate is made through the solder joint. The joint should be thin as possible for low thermal resistance and as soft as necessary to prevent strain. Typically, indium solder a few μm thick is used. This solder has drawbacks because it is difficult to remove indium oxides prior to bonding; its low melting point makes it difficult to establish a package soldering hierarchy; and In can alloy with Au or migrate under electrical or thermal gradients [36], thus presenting a potential long-term reliability problem. Nevertheless, for bonding lasers to substrates with significantly different linear expansion coefficients (such as Cu), the low melting point (165°C) and softness make it a necessary solder choice. Long life has been demonstrated using In solder [7]. Tin has also been successfully used as a solder in packages that bond lasers to expansion-matched substrates (such as Si or Mo) [32]. Tin solders are easier to clean than In and have higher melting temperatures, making them easier to incorporate into packaging processes.

The heat generated by the laser and its control and drive electronics must be dissipated by the package. We can estimate this heat load by determining the voltage drop necessary to drive and control the laser current through the device. (This assumes the other electronics in the module generate an insignificant amount of heat.) This drop is approximately the voltage drop across a drive transistor, a current-controlling resistor, and the laser itself, or $\approx$3-4 V. At drive currents up to 160 mA we may be generating 0.5-1.0 W of heat. Standard dual in-line package (DIP)-type ceramic modules can dissipate about 0.5 W with forced-air cooling [29], and more customized modules of about 2 cm dimension can dissipate over a watt. But the conclusion is that the laser does present a major heat load to the module and careful thermal design of the packaging is necessary. We note here that lower laser threshold currents and hence lower operating currents are important to the package thermal design and hence package cost.

Electrical contact is made through the p-side solder bond discussed above and an n-side flying lead. This two-side contacting is disadvantageous if the common side bonding techniques used in some electronics packaging are to be employed.

Conclusions

By comparing the current (GaAl)As double heterostructure laser with data network requirements we see that the injection laser is generally well suited in terms of performance. Its size is small; its optical output power is adequate; its beam shape, wavelength, and linewidth are matched to the transmission medium; its modulation speed is well matched to fiber bandwidths; and its reliability is expected to be acceptable for many applications. The thermal sensitivity of the optical output and the device reliability make the electrical drive circuitry more complicated and the packaging more critical than electronic chip packaging. Heat dissipation is a major concern in packaging today's laser. The edge emitting characteristic of the device and the optical components associated with laser-to-fiber coupling also make packaging issues critical, and an economic package has yet to be demonstrated. For the system designer, cost still remains a major deterrent. GaAs lasers are currently priced between a few hundred and a few thousand dollars. To the extent that manufacturing costs can be brought down to allow pricing comparable to electrical line driving and terminating costs, the use of lasers in optical data transmission systems will become widespread.

Acknowledgments

I thank my colleagues E. Lean and R. Lynch for encouragement in the preparation of this paper and review of its contents, and L. Comerford, D. Rogers, A. Widmer, and R. Hung for useful discussions.

References and notes

1. R. Kompfner, *Science* **150,** 149 (1965).
2. J. E. Geusic, W. B. Bridges, and J. I. Pankove, *Proc. IEEE* **58,** 1419 (1970).
3. F. P. Kapron, D. B. Keck, and R. D. Maurer, *Appl. Phys. Lett.* **17,** 423 (1970).
4. For a general review of fiber optic cables, see T. G. Giallorenzi, *Proc. IEEE* **66,** 744 (1978).
5. M. I. Nathan, W. P. Dumke, G. Burns, F. H. Dill, and G. Lasher, *Appl. Phys. Lett.* **1,** 62 (1962).
6. F. Hayashi, M. B. Pannish, P. W. Foy, and S. Sumski, *Appl. Phys. Lett.* **17,** 109 (1970).

7. R. L. Hartman, N. E. Schumaker, and R. W. Dixon, *Appl. Phys. Lett.* **31,** 756 (1977).
8. For a general review of semiconductor lasers, see H. C. Casey, Jr. and M. B. Pannish, *Heterostructure Lasers*, Academic Press, Inc., New York, 1978.
9. J. D. Crow and E. G. Lean, in *Proceedings of the First Fiber Optics and Communications Exposition* (Chicago, Sept. 6–8, 1978), M. A. O'Bryant and P. Polishuk, Eds., Information Gatekeepers, Inc., Brookline, MA, 1978, p. 148.
10. R. T. Lynch, Jr., M. B. Small, and R. Y. Hung, *IBM J. Res. Develop.* **23,** 585 (1979, this issue).
11. M. Ettenberg, H. Kressel, and I. Ladany, *Electron. Lett.* **14,** 815 (1978).
12. M. Ettenberg, *Appl. Phys. Lett.* **27,** 652 (1975).
13. E. Pinkas, *J. Appl. Phys.* **43,** 2827 (1972).
14. H. Kressel and J. K. Butler, *Semiconductor Lasers and Heterojunction LED's*, Academic Press, Inc., New York, 1977, p. 240.
15. W. P. Dumke, *Solid State Electron.* **16,** 1279 (1973).
16. B. W. Hakki, *J. Appl. Phys.* **46,** 292 (1975).
17. T. L. Paoli, *IEEE J. Quantum Electron.* **QE-12,** 770 (1976).
18. W. W. Benson, D. A. Pinnow, and T. C. Rich, *Appl. Opt.* **14,** 2815 (1975).
19. P. W. Shumate, Jr., J. S. Chen, and P. W. Dorman, *Bell Syst. Tech. J.* **57,** 1823 (1978).
20. J. D. Crow, L. D. Comerford, J. S. Harper, M. J. Brady, and R. A. Laff, *Appl. Opt.* **17,** 479 (1978).
21. C. K. Kao and J. E. Goell, "Design Process for Fiber Optic Systems Follows Familiar Rules," *Electronics*, September 16, 1976.
22. B. W. Hakki and F. R. Nash, *J. Appl. Phys.* **45,** 3907 (1974).
23. R. L. Hartman and R. W. Dixon, *Appl. Phys. Lett.* **26,** 239 (1975).
24. M. Ettenberg, H. S. Sommers, Jr., H. Kressel, and H. F. Lockwood, *Appl. Phys. Lett.* **18,** 571 (1971).
25. H. Imai, M. Morimoto, K. Hori, and M. Takusagawa, *Proc. IEEE/OSA Topical Meeting on Optical Fiber Communication*, Washington, DC, March 1979, paper ThB1.
26. T. Li, *IEEE Trans. Commun.* **COM-26,** 946 (1978).
27. R. Jarrett, *Electron. Design* **15,** 96 (1974).
28. T. C. Paoli, *Laser Focus* **13,** 54 (1977).
29. For example, see *MECL (Motorola Emitter Coupled Logic) System Design Handbook*, W. R. Blood, Jr. and E. C. Tynan, Jr., Eds., Motorola Semiconductor Products, Inc., Mesa, AZ.
30. R. A. Laff, L. D. Comerford, J. D. Crow, and M. J. Brady, *Appl. Opt.* **17,** 778 (1978).
31. A. R. Goodwin, J. R. Peters, M. Pion, G. H. B. Thompson, and J. E. A. Whiteaway, *J. Appl. Phys.* **46,** 3126 (1975).
32. H. Yonezu, T. Yuasa, T. Shinohara, T. Kamejima, and I. Sakuma, *Jpn. J. Appl. Phys.* **15,** 2393 (1976).
33. W. B. Joyce and R. W. Dixon, *J. Appl. Phys.* **46,** 885 (1975).
34. J. D. Crow, unpublished work.
35. Not unreasonable since R_{th} between the junction and a Cu heat sink is $\approx 25°C/W$; from there to a module package ambient should be $< 25°C/W$.
36. S. Ritchie, R. F. Godfrey, B. Wakefield, and D. H. Newman, *J. Appl. Phys.* **49,** 3127 (1978).
37. R. W. Dixon and R. L. Hartman, *J. Appl. Phys.* **48,** 3225 (1977).

Received February 22, 1979; revised May 2, 1979

The author is located at the IBM Thomas J. Watson Research Center, Yorktown Heights, New York 10598.